

Article

Compact and Wideband PIFA Design for Wireless Body Area Sensor Networks

Sandra Costanzo ^{1,2,3,4,*}  and Adil Masoud Qureshi ¹ 

- ¹ Dipartimento di Ingegneria Informatica, Modellistica, Elettronica e Sistemistica, Università della Calabria, 87036 Rende, Italy
- ² National Research Council of Italy (CNR), Institute for Electromagnetic Sensing of the Environment (IREA), 80124 Naples, Italy
- ³ ICeMB (Inter-University National Research Center on Interactions between Electromagnetic Fields and Biosystems), 16145 Genoa, Italy
- ⁴ CNIT (Consorzio Nazionale Interuniversitario per le Telecomunicazioni), 43124 Parma, Italy
- * Correspondence: costanzo@dimes.unical.it; Tel.: +39-0984-494652

Abstract: The specific advantage of fractal geometry to realize compact antenna features is exploited in this work for the design of a miniaturized Planar Inverted-F Antenna configuration with a large bandwidth. The conventional quadrilateral radiating element of a Planar Inverted-F Antenna is replaced by a Minkowski pre-fractal-based shape, thus increasing the resonant wavelength without affecting the overall antenna dimensions. Consequently, with the new design, a physically smaller antenna can achieve the same resonant frequency of a larger conventional configuration. Measured as well as simulated reflection coefficient and radiation patterns are presented to validate the assumptions. The impedance bandwidth of the antenna (2.19 to 2.52 GHz) covers the ISM band with a boresight gain of 1.5–2 dB over the entire band. Furthermore, to demonstrate the miniaturization effect, a successful comparison is provided with an identically sized, conventional square Planar Inverted-F Antenna design. The proposed antenna design can be usefully adopted for power-efficient communications in the framework of Wireless Body Area Sensor Networks.

Keywords: PIFA; compact antennas; WBAN



check for updates

Citation: Costanzo, S.; Qureshi, A.M. Compact and Wideband PIFA Design for Wireless Body Area Sensor Networks. *Electronics* **2021**, *10*, 2576. <https://doi.org/10.3390/electronics10212576>

Academic Editors: Syed Muzahir Abbas, Muhammad Ali Babar Abbasi and Leonardo Lizzi

Received: 26 July 2021
Accepted: 12 October 2021
Published: 21 October 2021

Publisher's Note: MDPI stays neutral with regard to jurisdictional claims in published maps and institutional affiliations.



Copyright: © 2021 by the authors. Licensee MDPI, Basel, Switzerland. This article is an open access article distributed under the terms and conditions of the Creative Commons Attribution (CC BY) license (<https://creativecommons.org/licenses/by/4.0/>).

1. Introduction

Planar Inverted-F antennas (PIFA) are arguably the most popular type of antenna and can be found in today's most popular personal communication devices [1]. The main reasons behind its widespread adoption are related to its compact size and appealing radiation features [2]. Even though it is electrically small, a PIFA is able to provide a relatively high gain, while maintaining the main radiation away from the user's body. Nevertheless, efforts to further miniaturize the PIFA have been ongoing in order to keep up with the rapid pace of development in the wider consumer electronics industry [3,4]. Constraints introduced by wearable applications such as Wireless Body Area Networks (WBAN) have renewed interest in innovative miniaturization techniques for PIFAs [5,6].

PIFAs are commonly designed to be part of circuit boards; therefore, the simplest miniaturization method is based on the adoption of a higher permittivity substrate material [7]. This technique cannot be used for WBAN antennas that are completely integrated into garments and clothing [8]. The use of exclusively textile-based materials makes it difficult to exploit substrate permittivity for miniaturization since high permittivity textile substrates are very rare [9]. Another technique deprecated by the wearable use-case is loading the PIFA with a capacitive or resistive impedance [10]. The reduction in radiation efficiency and bandwidth caused by impedance loading inhibits its use for wearable applications, where low power consumption and longer autonomy are paramount [5]. More refined approaches towards PIFA miniaturization have employed metamaterial ground

planes [11] or superstrates [12]. Even though these techniques promise good performance, the need for sophisticated manufacturing techniques and specialized materials limits their adoption in WBANs and other wearable applications. Apart from materials and manufacturability constraints, the antennas used in WBANs must also conform to strict regulatory requirements for the Specific Absorption Rate (SAR). This is essential to ensure that these devices can operate safely in close proximity to the human body for extended periods of time. The authors propose the use of fractal geometry to create compact and wideband antenna designs that are safe and that can be manufactured economically.

The potentiality of fractal shapes to reduce the resonant frequency of planar reflectarray elements has been recently demonstrated by the current authors [13]. A reduction in the resonant frequency while maintaining the physical size is equivalent to miniaturization [14]. Further preliminary works by the current authors have introduced the potential application of the above miniaturization effect to the PIFA configuration [15,16].

In the present work, a detailed analysis of the idea originally proposed in [15,16] is presented by reporting the full design principle and by discussing the validation results in terms of both simulations as well as experimental tests. The actual radiation performance of the proposed miniaturized PIFA configuration is successfully compared with that relative to the conventional square-shaped PIFA design. As a further result, the adoption of a defected ground plane is exploited to obtain a significant enhancement (around 14%) in terms of the operation bandwidth.

2. Antenna Design

The conventional PIFA consists of a rectangular/square radiating element/patch mounted on a ground plane. The radiating element is connected to the ground plane via a shorting plate (or post/via). In the case of a square radiating element on side “S” and a shorting plate of length “L”, the resonant frequency can be estimated as:

$$\lambda = 4 \times \epsilon_r^{1/2} \times (2S - L), \quad (1)$$

Expression (1) is not always accurate since the resonant frequency depends on the feed location as well as on the shape and the size of the ground plane. However, it can be observed that the resonant frequency is related to the length of the current path around the edge of the radiating element from the short to the open circuit end. By increasing the length of the current path, the antenna can be led to operate at a lower frequency; however, an increase in the perimeter of a quadrilateral results in a corresponding rise in the antenna footprint.

To overcome the above issue, fractal geometry is adopted in the present work. Fractals are unique structures, meaning that the perimeter of a fractal is not rigidly coupled with its area. By introducing a pre-fractal shape, the perimeter of the radiating element can be enlarged without augmenting the footprint. To create the pre-fractal Minkowski, rectangular sections are cut out from each edge of the square radiating element (see Figure 1). The increase in the perimeter of the radiating element depends on the dimensions of the above rectangles.

The design process starts from the classical PIFA with a square radiating element. The Minkowski generator is applied to each side of this square, yielding a first iteration Minkowski pre-fractal. This is followed by an iterative optimization process in which the depth “D” and width “W” of the slots are adjusted to achieve the desired operational frequency. The position of the probe feed is also optimized to achieve a good impedance match. The impedance bandwidth of the PIFA is directly related to the substrate thickness or the height of the radiating element above the ground plane. However, indefinitely increasing the profile of an antenna is not always desirable. Therefore, the authors have utilized a defected ground plane technique, which is described in subsequent sections to achieve the maximum possible bandwidth without increasing substrate (air in the present case) thickness.

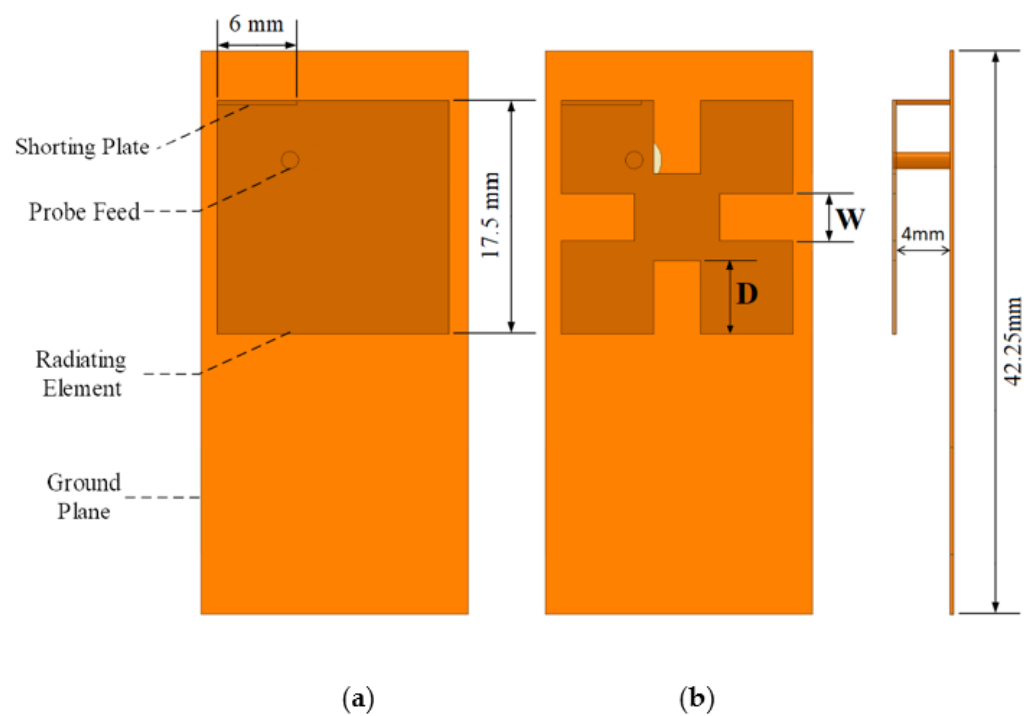


Figure 1. (a) Conventional square-shaped PIFA element, and (b) Minkowski pre-fractal-shaped PIFA element.

2.1. Simulation Results

Both the square and the pre-fractal Minkowski antennas shown in Figure 1 are simulated using 3D EM simulation software. Each radiating element is placed 4 mm above a 20.25×42.25 mm ground plane. The models are created on air substrate, and the radiating elements are fed using a standard coaxial probe feed. The shorting plate for both of the antenna models is 6 mm long. The feed position, however, is optimized separately for each antenna.

The simulated reflection coefficient [17], for the square and the Minkowski pre-fractal PIFA, is reported in Figure 2. The square PIFA resonates at around 2.7 GHz, while the Minkowski pre-fractal PIFA's resonant frequency can be tuned by changing the dimensions of the rectangular cut-outs. Figure 2 shows the results for the initial variant, with a cut-out size equal to $4 \text{ mm} \times 4 \text{ mm}$, which exhibits a resonant frequency at 2.36 GHz.

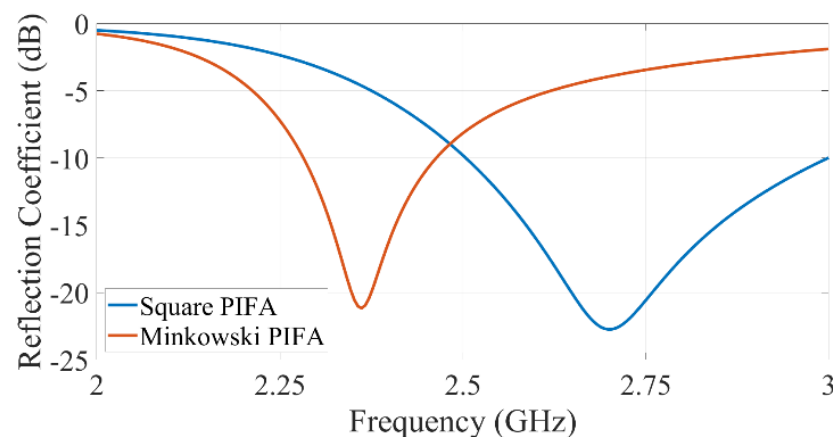


Figure 2. Simulated reflection coefficient: comparison between the Minkowski pre-fractal-shaped PIFA and the conventional square PIFA design.

Since both antennas have the same overall size, the lower resonant frequency corresponds to a 12.5% reduction in size. Notwithstanding the physical transformation of the radiating element, the radiation patterns remain unchanged. However, a side effect of the applied miniaturization process can be observed in terms of reduction in the impedance bandwidth. In particular, the fractional frequency band of the square element PIFA is over 17%, whereas the miniaturized PIFA from Figure 1b offers a bandwidth value under 8%.

2.2. Parametric Analysis

As previously remarked, the resonant frequency is a function of the current path around the boundary of the radiating element. When using the pre-fractal geometry, the path length, and therefore the resonant frequency, is related to the size of the cut-outs. In order to verify this point, a parametric analysis is conducted by varying the depth “D” and the width “W” (Figure 1). Figure 3 shows the reflection coefficient of the Minkowski pre-fractal PIFA for different values of the depth “D”. The indentation width “W” as well as all other design parameters, including the feed position, are unchanged. It can be clearly seen that the resonant frequency of the antenna decreases with an increase in the depth “D”. This is consistent with the fact that the perimeter “P” of the pre-fractal radiating element is equal to $4 \times (S + 2D)$. The maximum depth “D”, which is equal to 6 mm, yields a resonant frequency of around 2.17 GHz, corresponding to a miniaturization of about 20%.

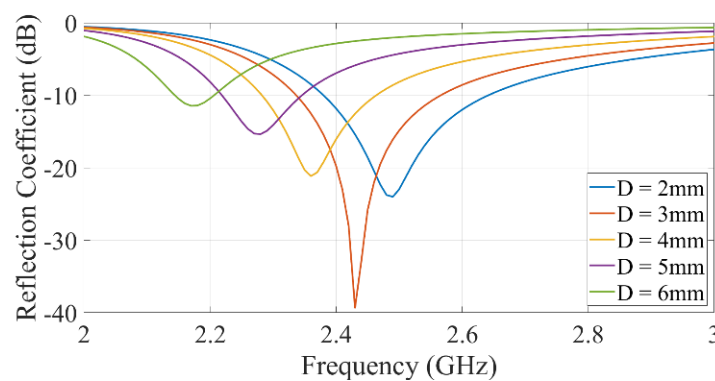


Figure 3. Simulated reflection coefficient of the proposed PIFA design for different slot depths.

On the other hand, the width “W” of the slots does not add to the length of the current path; therefore, it is not expected to affect the resonant frequency. This is confirmed by the results of the parametric analysis illustrated in Figure 4, where different values are assumed in simulations for the width “W”. In particular, it can be observed that the resonant frequency of the antenna remains almost unchanged. The only discernable difference can be seen in the quality factor Q.

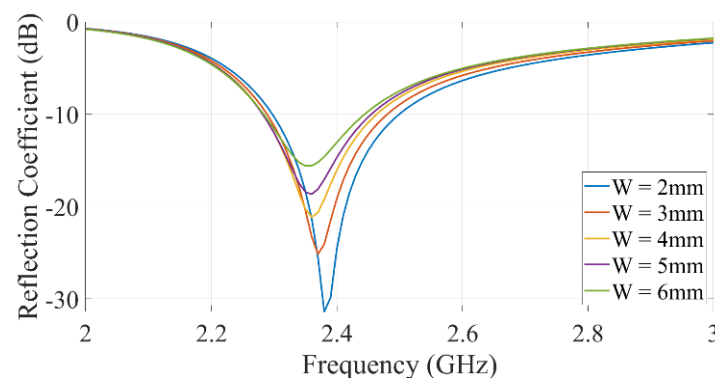


Figure 4. Simulated reflection coefficient of the proposed PIFA design for different notch widths.

2.3. Bandwidth Enhancement

A larger usable bandwidth is desirable, as it offers protection against detuning while further enabling higher data rate communication. The bandwidth of a PIFA as well as its radiation pattern is deeply influenced by the size of the ground plane [18]. For example, Wu and Wong [19] show that the impedance bandwidth of the PIFA is maximized at a length of around 0.45λ . This is confirmed by Bohannon and Bernhard [20], and it is explained on the basis of multiple characteristic modes with close enough resonances [21]. At the resonant frequency of 2.36 GHz, for the Minkowski pre-fractal-shaped PIFA, the ground plane length of 42.25 mm is around 0.33λ . Increasing the length of the ground plane to 0.45λ for optimum bandwidth would defeat the initial goal of miniaturization. Fortunately, it is possible to simulate a longer ground plane by using a defected ground plane. Wang et al. [22] have shown that it is possible to achieve a “bandwidth maxima” with a fixed length ground plane using a T-shaped modification. Figure 5 shows the simulated reflection coefficient of the proposed Minkowski pre-fractal PIFA with the adoption of a T-shaped ground plane. The final design, with $W = 3.5$ mm and $D = 5.5$ mm, is a significant improvement over the initial miniaturized design. The simulated reflection coefficient is lower than -10 dB, from 2.19 GHz to 2.52 GHz, corresponding to a 14% fractional impedance bandwidth.

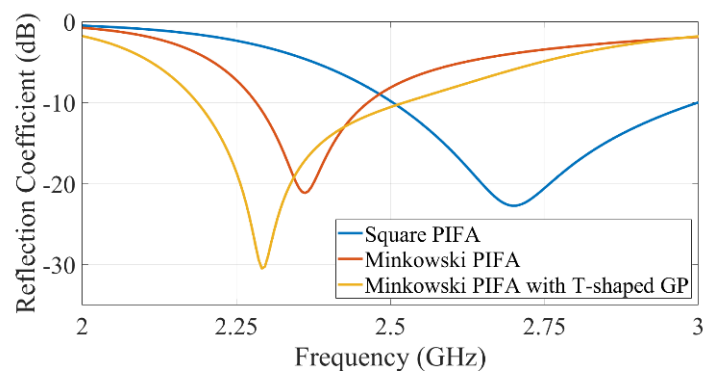


Figure 5. Simulated reflection coefficient for the Minkowski-pre-fractal-shaped PIFA (with and without T-shaped ground plane) compared to the original Square PIFA design.

2.4. Radiation Pattern

The radiation performance of the miniaturized antenna is on par with the classical square-shaped PIFA element. Figure 6 shows a comparison of the simulated radiation patterns for both the miniaturized antenna and the original PIFA in the E and H planes. A minor reduction in gain, about 0.55 dB at boresight, compared to the original square PIFA was observed in the simulated results. This is to be expected since gain is influenced by the electrical size of the antenna, which in the case for the Minkowski pre-fractal-shaped PIFA, which has been reduced by around 12.5%.

2.5. On Body Performance and SAR Analysis

Simulations were conducted using CST Microwave Studio to evaluate the on-body performance of the antenna and its compliance with safety regulations. In order to mimic the human body, a multilayer phantom was used, with different layers representing skin, fat, and muscle, etc. [23]. A reduction in the resonant frequency of the antenna was observed due to proximity to the high permittivity body tissues (Figure 7), whose properties are reported in Table 1. This can easily be resolved by scaling down the physical dimensions of the antenna even further and by re-optimizing the feed position. The resulting antenna has a slightly reduced impedance bandwidth (2.26 to 2.52 GHz); nevertheless, the ISM band (2.4–2.5 GHz) is still covered.

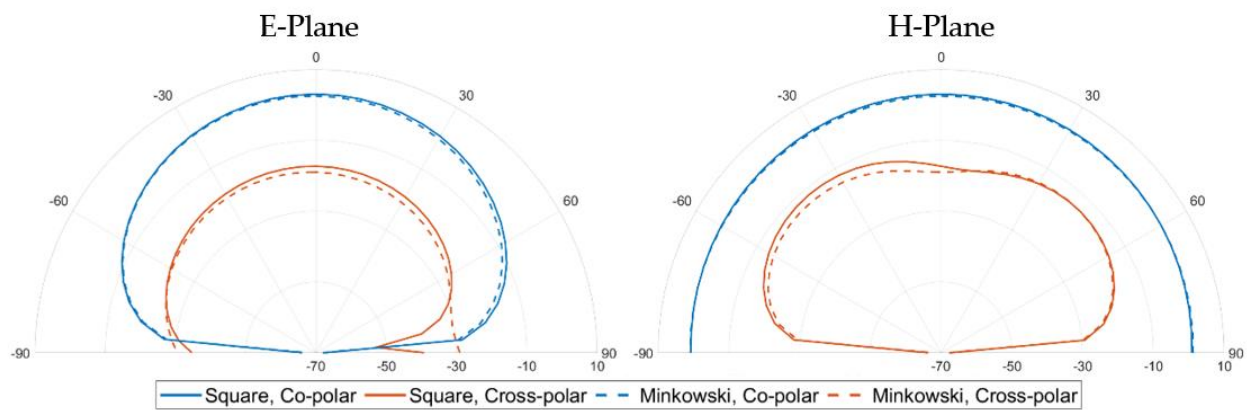


Figure 6. Simulated radiation pattern for the Minkowski pre-fractal-shaped PIFA (with T-shaped ground plane) compared to the original Square PIFA design.

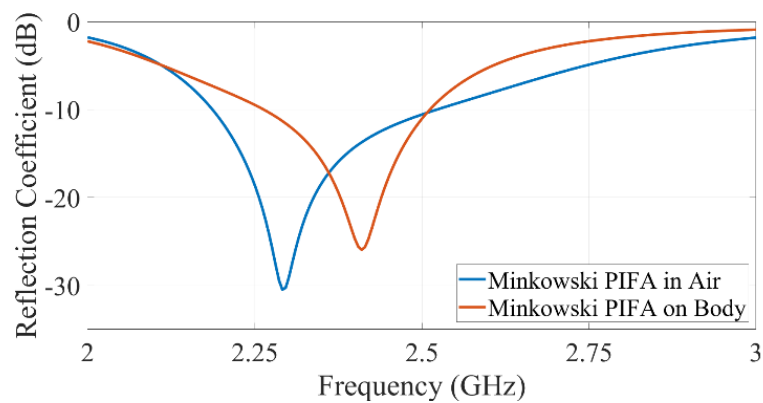


Figure 7. Simulated reflection coefficient for the Minkowski pre-fractal-shaped PIFA in air and placed on the human body.

Table 1. Dielectric Properties of Body Tissue [24–26].

| Tissue Type | Relative Permittivity (ϵ_r) | Loss Tangent ($\tan\delta$) |
|-------------|----------------------------------------|-------------------------------|
| Skin | 38.06 | 0.28 |
| Fat | 5.28 | 0.14 |
| Muscle | 52.79 | 0.24 |

Figure 8 presents a comparison of the simulate radiation patterns of the Minkowski pre-fractal-shaped PIFA antenna while it is suspended in air and when it is placed on the human body. A slight reduction in gain can be observed, which is caused by the lossy high permittivity body tissue. The major impact of being in proximity to the human body can be seen on the increased cross-polar radiation levels. Despite the marked increase, cross-polar isolation remains better than 10 dB within the beamwidth of the antenna.

The results show (Figure 9) that the maximum specific absorption rate (SAR) averaged over 10 g of body tissue is about 9.6 W/Kg for the Minkowski pre-fractal-shaped PIFA. In order to improve the SAR performance, the ground plane was extended by 5 mm on three sides, leading to an overall ground plane size of 33.75 mm × 30.25 mm. The extension of the ground plane led to a drastic reduction in the SAR value, to a level of 2.91 W/Kg. Thus, the SAR level of the proposed antenna is well under the existing European [27] and North American [28] standards for devices worn on limbs (arms, legs, etc.), which is 4 W/Kg. The simulated on-body radiation efficiency of the antenna is over 60%.

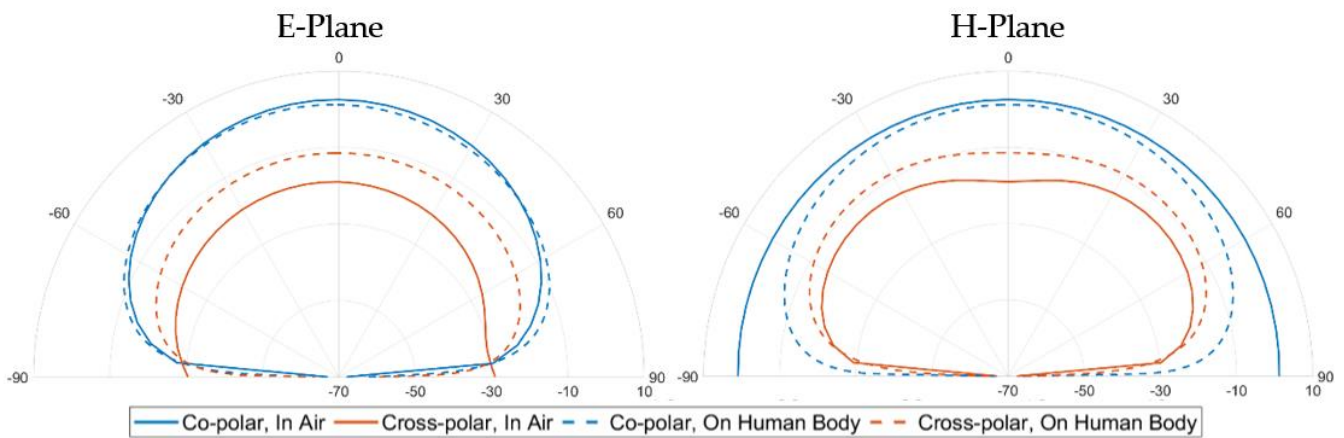


Figure 8. Simulated radiation pattern for the Minkowski pre-fractal-shaped PIFA placed on human body tissue compared to the Minkowski pre-fractal-shaped PIFA in air.

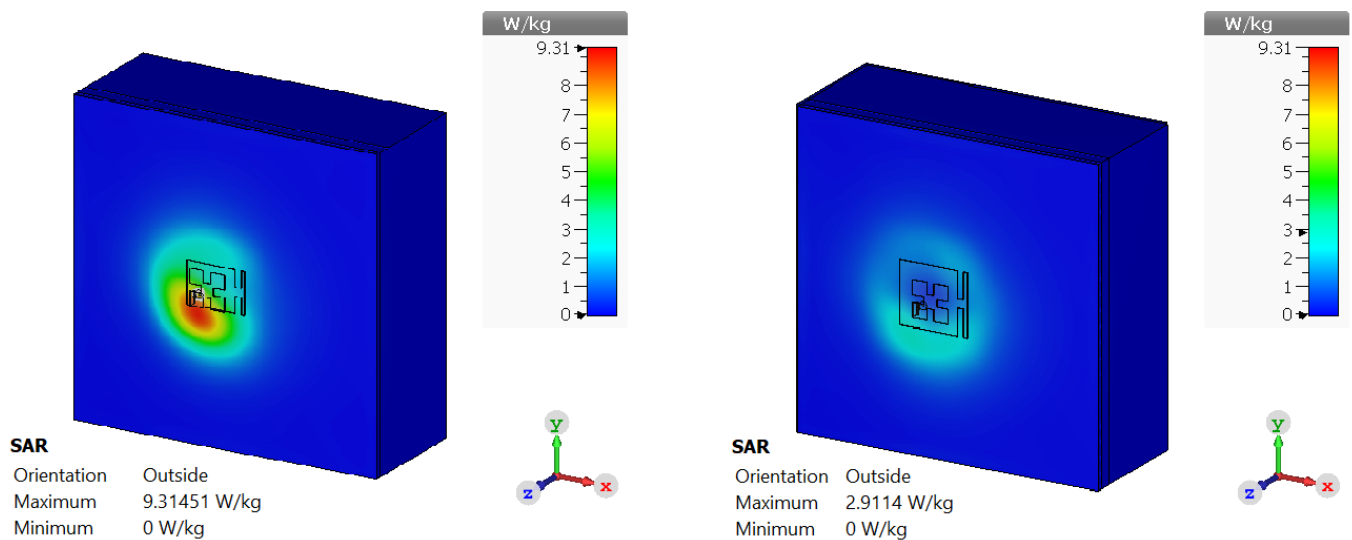


Figure 9. SAR simulation for the Minkowski pre-fractal-shaped PIFA in the presence of human body tissue.

2.6. Comparison with Other Miniaturized PIFAs

Table 2 presents a brief comparison of the designed antenna with other miniaturized PIFAs present in the literature. It can be observed that the proposed antenna is considerably smaller while offering comparable performance.

Table 2. Comparison with other designs.

| Reference | Radiating Element Length | Radiating Element Width | Ground Plane Length | Ground Plane Width | Substrate Height | Fractional Bandwidth (%) | Gain (dBi) |
|-----------------------|--------------------------|-------------------------|---------------------|--------------------|------------------|--------------------------|------------|
| This paper | 0.14 λ | 0.14 λ | 0.33 λ | 0.16 λ | 0.031 λ | 14 | 2.6 |
| Guterman et al. [29] | 0.15 λ | 0.24 λ | 0.67 λ | 0.30 λ | 0.077 λ | 17.5 | 3.0 |
| Soh et al. [30] | 0.22 λ | 0.32 λ | 0.40 λ | 0.32 λ | 0.055 λ | 16 | 3.1 |
| Saidatu et al. [31] | 0.18 λ | 0.18 λ | No data | No data | 0.053 λ | 20 | 2.8 |
| Elfergani et al. [32] | 0.16 λ | 0.10 λ | 0.59 λ | 0.31 λ | 0.037 λ | 8.5 | 2.4 |
| Gao et al. [12] | 0.39 λ | 0.55 λ | 0.77 λ | 0.51 λ | 0.070 λ | 18 | 6.7 |
| Khan et al. [33] | 0.09 λ | 0.09 λ | 0.51 λ | 0.27 λ | 0.055 λ | 7.5 | 2.8 |
| Ghazali et al. [34] | 0.17 λ | 0.17 λ | 1.65 λ | 0.88 λ | No data | No data | 6.7 |

3. Experimental Results

The conventional PIFA antenna with a square radiating element and the Minkowski pre-fractal PIFA antenna with a T-shaped ground plane were manufactured in the Microwave Laboratory at the University of Calabria. A 300-micron copper sheet was used to fabricate the ground plane and the radiating elements, while the probe feed was replaced by an SMA connector soldered on to the back of the ground plane. The reflection coefficient and gain measurements were conducted in an anechoic chamber in order to compare the performance of the two antennas. Figure 10 shows the manufactured prototypes along with a 50 cent (EUR) coin for size comparison. Due to the lack of a suitable human body phantom and test fixture, the on-body variant could not be tested at present but will be included in future contributions.

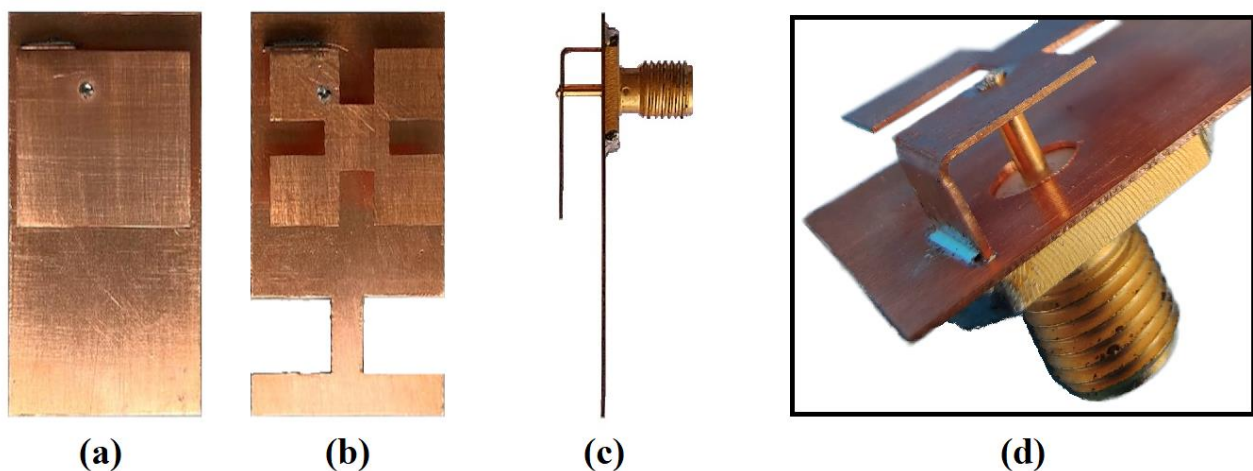


Figure 10. Photograph of the manufactured square (a) and Minkowski (b) PIFAs along with a side view (c) and details of probe feed and shorting plate (d).

Overall, good agreement is obtained between the experimental and the simulation results (Figure 11). Variations in the resonant frequency are very small, less than 1%, which are likely to be due to acceptable tolerances in the fabrication process. The square PIFA is resonant at 2.73 GHz, while the Minkowski pre-fractal design resonates at a frequency equal to 2.34 GHz. When comparing the simulations, a very small reduction in the measured bandwidth can be appreciated for both antennas.

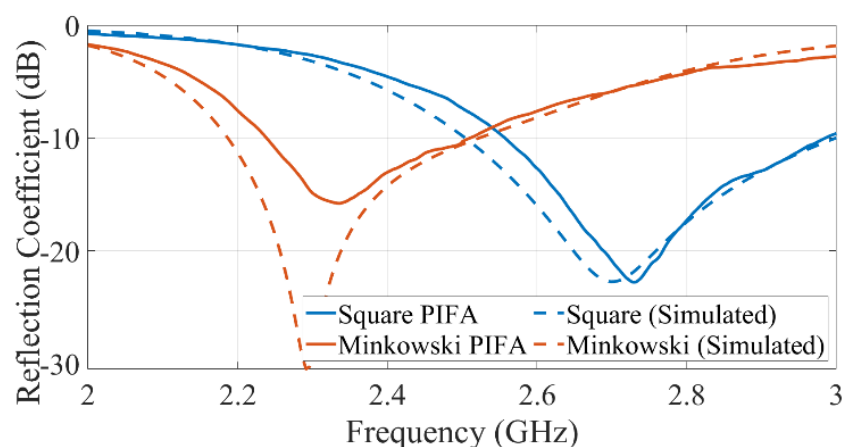


Figure 11. Comparison of measured and simulated reflection coefficient for the manufactured prototypes.

Boresight gain measurements were also conducted for both of the realized antennas in the anechoic chamber of the Microwave Laboratory at the University of Calabria. The

two antenna methods were adopted by using a standard log-periodic antenna as a reference (Figure 12).



Figure 12. Measurement setup for PIFA gain measurements (anechoic chamber at the Microwave Laboratory of the University of Calabria) along with the definition of the E and H planes.

Figure 13 shows a comparison between the measured and simulated boresight gains for each of the manufactured PIFA prototypes. Although the measured values follow the same general pattern as the simulations, a better agreement is observed within the usable bandwidth of each antenna. Outside of the above band, the measured gains slightly taper away from the simulated results.

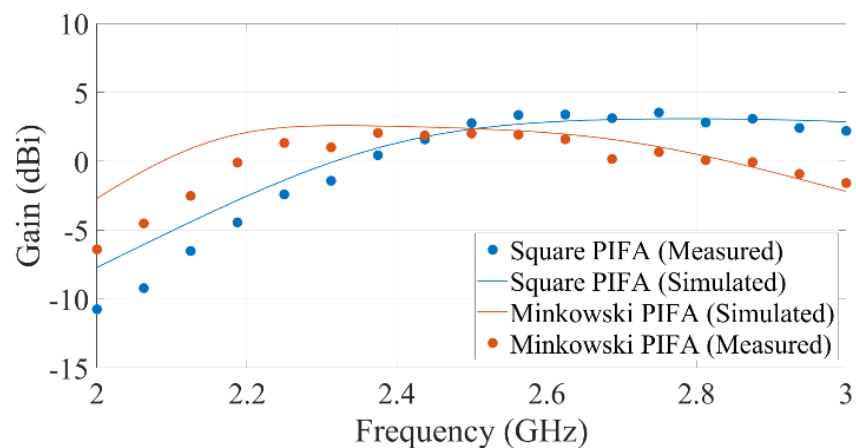


Figure 13. Comparison of measured and simulated gains for the square PIFA and Minkowski pre-fractal-shaped PIFA.

The measured radiation patterns of the Minkowski pre-fractal-based PIFA design are compared with the simulated results in Figure 14. The measured co-polar radiation pattern shows very good agreement with the simulated pattern, especially in the vicinity of the boresight. The cross-polar radiation pattern tends to exceed the levels expected from the simulations as the receiver moves away from boresight. Nevertheless, a cross-polar isolation of >10 dB is maintained, which is within the 3 dB beamwidth of the antenna.

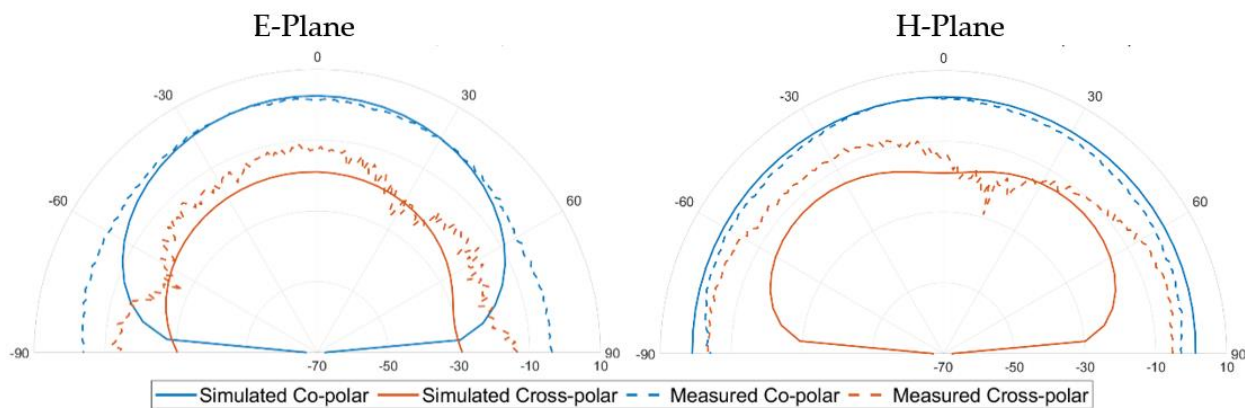


Figure 14. Comparison of measured and simulated radiation patterns for the Minkowski pre-fractal-based PIFA design in the E and H planes at 2.34 GHz.

4. Conclusions

A fractal-based design for a miniaturized Planar Inverted-F Antennas was introduced. By modifying the shape of the radiating element, the antenna was designed to resonate at a lower frequency than a standard PIFA with the same size. Despite miniaturization, the radiation pattern and usable impedance bandwidth were well preserved by also exploiting the benefits achieved with the adoption of a defected ground plane. The proposed design offers potential applications where space-saving solutions are required, such as in the framework of wireless body area networks.

Author Contributions: Conceptualization, S.C.; methodology, S.C.; software, A.M.Q.; validation, A.M.Q.; formal analysis, A.M.Q.; investigation, A.M.Q.; resources, S.C.; data curation, S.C.; writing—original draft preparation, A.M.Q.; writing—review and editing, S.C.; visualization, A.M.Q.; supervision, S.C.; project administration, S.C.; funding acquisition, S.C.; All authors have read and agreed to the published version of the manuscript.

Funding: This research received no external funding.

Acknowledgments: The authors would like to thank Ing. Antonio Borgia for the generous technician support in the realization of the prototypes and the realization of the measurements.

Conflicts of Interest: The authors declare no conflict of interest.

References

1. Fujimoto, K. (Ed.) *Mobile Antenna Systems Handbook*, 3rd ed.; Artech House: Boston, MA, USA, 2008.
2. Vaughan, R.; Bach-Anderson, J. *Channels, Propagation and Antennas for Mobile Communications*; Institution of Engineering and Technology: London, UK, 2003.
3. Rothwell, E.J.; Ouedraogo, R.O. Antenna miniaturization: Definitions, concepts, and a review with emphasis on metamaterials. *J. Electromagn. Waves Appl.* **2014**, *28*, 2089–2123. [[CrossRef](#)]
4. Fallahpour, M.; Zoughi, R. Antenna Miniaturization Techniques: A Review of Topology- and Material-Based Methods. *IEEE Antennas Propag. Mag.* **2018**, *60*, 38–50. [[CrossRef](#)]
5. Dumanli, S. Challenges of wearable antenna design. In Proceedings of the 2016 11th European Microwave Integrated Circuits Conference (EuMIC), London, UK, 3–4 October 2016; pp. 421–423. [[CrossRef](#)]
6. Rais, N.H.M.; Soh, P.J.; Malek, F.; Ahmad, S.; Hashim, N.B.M.; Hall, P.S. A review of wearable antenna. In Proceedings of the 2009 Loughborough Antennas & Propagation Conference, Loughborough, UK, 16–17 November 2009; pp. 225–228. [[CrossRef](#)]
7. Lo, T.K.-C.; Hwang, Y. Bandwidth enhancement of PIFA loaded with very high permittivity material using FDTD. In Proceedings of the IEEE Antennas and Propagation Society International Symposium. 1998 Digest. Antennas: Gateways to the Global Network. Held in conjunction with: USNC/URSI National Radio Science Meeting (Cat. No.98CH36), Atlanta, GA, USA, 21–26 June 1998; Volume 2, pp. 798–801. [[CrossRef](#)]
8. van Langenhove, L.; Hertleer, C.; Schwarz, A. Smart Textiles: An Overview. In *Intelligent Textiles and Clothing for Ballistic and NBC Protection*; Kiekens, P., Jayaraman, S., Eds.; Springer: Dordrecht, The Netherlands, 2012; pp. 119–136. [[CrossRef](#)]
9. Salvado, R.; Loss, C.; Gonçalves, R.; Pinho, P. Textile Materials for the Design of Wearable Antennas: A Survey. *Sensors* **2012**, *12*, 15841–15857. [[CrossRef](#)] [[PubMed](#)]

10. Waterhouse, R.B. (Ed.) *Printed Antennas for Wireless Communications*; Wiley: Chichester, UK; Hoboken, NJ, USA, 2007.
11. Gao, G.; Hu, B.; Wang, S.; Yang, C. Wearable planar inverted-F antenna with stable characteristic and low specific absorption rate. *Microw. Opt. Technol. Lett.* **2018**, *60*, 876–882. [[CrossRef](#)]
12. Gao, G.; Yang, C.; Hu, B.; Zhang, R.; Wang, S. A Wearable PIFA with an All-Textile Metasurface for 5 GHz WBAN Applications. *IEEE Antennas Wirel. Propag. Lett.* **2019**, *18*, 288–292. [[CrossRef](#)]
13. Costanzo, S.; Venneri, F. Miniaturized Fractal Reflectarray Element Using Fixed-Size Patch. *IEEE Antennas Wirel. Propag. Lett.* **2014**, *13*, 1437–1440. [[CrossRef](#)]
14. Oloumi, D.; Ebadi, S.; Kordzadeh, A.; Semnani, A.; Mousavi, P.; Gong, X. Miniaturized Reflectarray Unit Cell Using Fractal-Shaped Patch-Slot Configuration. *IEEE Antennas Wirel. Propag. Lett.* **2012**, *11*, 10–13. [[CrossRef](#)]
15. Costanzo, S.; Qureshi, A.M. Miniaturized Wearable Minkowski Planar Inverted-F Antenna. In Proceedings of the 2020 International Conference on Information Technology & Systems (ICITS'20), Bogota, Colombia, 5–7 February 2020.
16. Coo, S.; Qureshi, A.M. Miniaturized Planar Inverted-F Antenna using Minkowski Pre-Fractal Structure. In Proceedings of the 14th European Conference on Antennas and Propagation (EuCAP), Copenhagen, Denmark, 15–20 March 2020.
17. Bird, T.S. Definition and Misuse of Return Loss [Report of the Transactions Editor-in-Chief]. *IEEE Antennas Propag. Mag.* **2009**, *51*, 166–167. [[CrossRef](#)]
18. Huynh, M.-C.; Stutzman, W. Ground plane effects on planar inverted-F antenna (PIFA) performance. *Antennas Propag. IEEE Proc.-Microw.* **2003**, *150*, 209–213. [[CrossRef](#)]
19. Wu, T.; Wong, K. On the impedance bandwidth of a planar inverted-f antenna for mobile handsets. *Microw. Opt. Technol. Lett.* **2002**, *32*, 249–251. [[CrossRef](#)]
20. Bohannon, N.L.; Bernhard, J.T. Design Guidelines Using Characteristic Mode Theory for Improving the Bandwidth of PIFAs. *IEEE Trans. Antennas Propag.* **2015**, *63*, 459–465. [[CrossRef](#)]
21. Bohannon, N.L.; Bernhard, J.T. Ground plane effects on planar inverted-F antennas. In Proceedings of the 2012 IEEE International Symposium on Antennas and Propagation, Chicago, IL, USA, 8–14 July 2012; pp. 1–2. [[CrossRef](#)]
22. Wang, F.; Du, Z.; Wang, Q.; Gong, K. Enhanced-bandwidth PIFA with T-shaped ground plane. *Electron. Lett.* **2004**, *40*, 1504–1505. [[CrossRef](#)]
23. Gao, G.-P.; Yang, C.; Hu, B.; Zhang, R.-F.; Wang, S.-F. A Wide-Bandwidth Wearable All-Textile PIFA With Dual Resonance Modes for 5 GHz WLAN Applications. *IEEE Trans. Antennas Propag.* **2019**, *67*, 4206–4211. [[CrossRef](#)]
24. Gabriel, S.; Lau, R.W.; Gabriel, C. The dielectric properties of biological tissues: II. Measurements in the frequency range 10 Hz to 20 GHz. *Phys. Med. Biol.* **1996**, *41*, 2251–2269. [[CrossRef](#)]
25. Gabriel, S.; Lau, R.W.; Gabriel, C. The dielectric properties of biological tissues: II. Measurements in the frequency range 10 Hz to 20 GHz. *Phys. Med. Biol.* **1996**, *41*, 2271–2293. [[CrossRef](#)]
26. Dielectric Properties of Body Tissues: HTML Clients. Available online: <http://niremf.ifac.cnr.it/tissprop/htmlclie/htmlclie.php> (accessed on 11 October 2021).
27. TDCA (Trade, Development and Cooperation Agreement). Official Journal of the European Communities, L 311/3. 1999. Available online: <https://eur-lex.europa.eu/LexUriServ/LexUriServ.do?uri=OJ:L:1999:311:SOM:EN:HTML> (accessed on 20 April 2021).
28. Available online: <https://www.fcc.gov/search/#q=specific%20absorption%20rate&t=web> (accessed on 26 July 2021).
29. Guterman, J.; Moreira, A.A.; Peixeiro, C. Microstrip fractal antennas for multistandard terminals. *IEEE Antennas Wirel. Propag. Lett.* **2004**, *3*, 351–354. [[CrossRef](#)]
30. Soh, P.J.; Vandenbosch, G.A.E.; Ooi, S.L.; Husna, M.R.N. Wearable dual-band Sierpinski fractal PIFA using conductive fabric. *Electron. Lett.* **2011**, *47*, 365–367. [[CrossRef](#)]
31. Saidatul, N.A.; Azremi, A.A.H.; Ahmad, R.B.; Soh, P.J.; Malek, F. Multiband Fractal Planar Inverted F Antenna (F-PIFA) for Mobile Phone Application. *PIER B* **2009**, *14*, 127–148. [[CrossRef](#)]
32. Elfergani, I.T.; Abd-Alhameed, R.; See, C.H.; Sadeghpour, T.; Dama, Y.; Jones, S.; Excell, P. A compact size reconfigurable PIFA antenna for use in mobile handset. In Proceedings of the 2011 XXXth URSI General Assembly and Scientific Symposium, Istanbul, Turkey, 13–20 August 2011; pp. 1–4. [[CrossRef](#)]
33. Khan, M.M.; Hossain, T. Compact Planar Inverted F Antenna (PIFA) for Smart Wireless Body Sensors Networks. *Eng. Proc.* **2020**, *2*, 63. [[CrossRef](#)]
34. Ghazali, M.I.M.; Karuppuswami, S.; Mondal, S.; Chahal, P. A 3D Printed Compact PIFA for 5G Applications. In Proceedings of the 2019 IEEE International Symposium on Antennas and Propagation and USNC-URSI Radio Science Meeting, Atlanta, GA, USA, 7–12 July 2019; pp. 1995–1996. [[CrossRef](#)]